Aquaporin-2 Transfection of Madin-Darby Canine Kidney Cells Reconstitutes Vasopressin-Regulated Transcellular Osmotic Water Transport

PETER M. T. DEEN, JOHAN P. L. RIJSS, SABINE M. MULDERS, RACHEL J. ERRINGTON, JÜRGEN VAN BAAL, and CAREL H. VAN OS
Department of Cell Physiology, University of Nijmegen, Nijmegen, The Netherlands.

Abstract. Water transport across the mammalian collecting tubule is regulated by vasopressin-dependent aquaporin-2 insertion into and retrieval from the apical cell membrane. To establish a cell line that properly expresses aquaporin-2 and its hormone-dependent shuttling, Madin-Darby canine kidney cells were stably transfected with an aquaporin-2 expression construct. Cells of a representative clone (wild-type 10 [WT-10]) were grown on semipermeable supports, and transcellular osmotic water permeability (Pf; in μm/s $\pm$ SEM) was measured. The basal Pf of WT-10 cells, which was lowered with indomethacin, increased from 10.6 $\pm$ 0.8 to 35.7 $\pm$ 1.2 upon incubation with 1-desamino-8-D-arginine vasopressin (dDAVP). This increase coincided with the translocation of aquaporin-2 from an intracellular compartment to the apical membrane. The Pf of untransfected cells (6.5 $\pm$ 0.8) was unchanged by dDAVP. Kinetic studies with WT-10 cells revealed that maximal Pf was obtained within 30 min after dDAVP addition, which remained elevated for at least 90 min. Intracellular cAMP levels peaked within 5 min after dDAVP admission and decreased to basal levels within 45 min. After preincubation with dDAVP, the Pf decreased within 15 min after dDAVP washout and returned to basal levels within 75 min. In conclusion, the WT-10 cells mimic the vasopressin-regulated transcellular water transport and aquaporin-2 translocation as found in collecting duct cells to a great extent, and therefore constitute an *in vitro* cell model that can be used to study the regulation of transcellular water transport in detail and provide a simplified test system for screening putative aquaporin-2 blockers. (J Am Soc Nephrol 8: 1493–1501, 1997)

Since the identification of the first mammalian water channel, the channel-forming integral membrane protein of 28 kD (CHIP28), or aquaporin-1 (AQP-1), the aquaporin family in mammals has been expanded to six members and is likely to grow (reviewed in references 1 and 2). In general, aquaporins are intrinsic membrane proteins of approximately 30 kD that form channels and facilitate selective water transport across cell membranes. For most aquaporins, this water permeability can be blocked by sulfhydryl reagents, which is due to binding of mercury to a cysteine amino acid present in an extracellular loop, thought to be near the mouth of the water pore (3,4).

Although mammalian aquaporins are very similar in primary structure, they differ greatly in tissue distribution, subcellular localization, and regulation of expression (1,2). In the kidney, four aquaporins (AQP-1, AQP-2, AQP-3, and AQP-4) are expressed. AQP-1 is constitutively and abundantly expressed in the apical and basolateral membranes of epithelial cells lining renal proximal tubules and descending limbs of Henle (reviewed in reference 5). Extensive evidence has recently accumulated indicating that AQP-2, which is exclusively expressed in principal and inner medullary collecting duct cells, is the vasopressin-regulated water channel (6–8). It is now widely accepted that the hormone arginine vasopressin (AVP) binds to V2 receptors, present on the basolateral plasma membrane of principal and inner medullary collecting duct cells. Transduction of the signal results in elevated intracellular cAMP levels, which eventually trigger the fusion of intracellular vesicles, containing AQP-2 water channels, with the apical membrane. Because this membrane is the rate-limiting barrier for water flow, this action renders the cells water-permeable. Removal of AVP induces endocytosis of AQP-2 in clathrin-coated vesicles, restoring the water-impermeable state of the cells. AQP-3 and AQP-4 are expressed at the basolateral membranes of these cells and might form the exit pathway for water entered through AQP-2 (9,10).

Of the four aquaporins expressed in kidney, only the clinical importance of AQP-2 has been shown convincingly, because mutations in the *AQP-2* gene have been shown to cause the autosomal recessive form of nephrogenic diabetes insipidus (NDI) (11,12). Upon expression in oocytes, these naturally occurring AQP-2 mutants were impaired in their cellular routing (13,14). In addition, secondary NDI in rats, induced by well-recognized causes such as lithium therapy, chronic hypokalemia, and bilateral ureteral obstruction, correlated with dra-

Received January 16, 1997. Accepted May 2, 1997.
Correspondence to Dr. Peter M. T. Deen, Department 162, Cell Physiology, University of Nijmegen, P. O. Box 9101, 6500 HB Nijmegen, The Netherlands.
1046-6673/08010-1493$03.00/0
Journal of the American Society of Nephrology

matically reduced AQP-2 expression and disturbed AQP-2 distribution within the cell (15–17).

To be able to delineate the molecular causes underlying primary and secondary NDI and to obtain a simple test system for AQP-2 blockers to be used as aquaretics, a cell line that properly expresses AQP-2 and its hormone-dependent shuttling would be desirable. No cell line with endogenous AQP-2 expression is known. In transfected renal pig cells (LLC-PK1; American Type Culture Collection no. CL-101), vasopressin-regulated cycling of AQP-2 was shown to occur at the wrong side of the cell (18,19). During our study, Valenti *et al.* reported vasopressin-dependent apical routing of AQP-2 in a transfected cell line, but the kinetics of insertion of AQP-2 in the apical membrane and transcellular water permeabilities were not determined (20). In the present study, Madin-Darby canine kidney (MDCK) cells, which have an extremely low water permeability at the apical side and which express functional V2 receptors (21,22), were transfected with an *AQP-2* expression construct. In these transfected cells, we could show that the V2 receptor-specific AVP analogue 1-desamino-8-D-arginine vasopressin (dDAVP) induced transcellular osmotic water flow, which coincided with the translocation of AQP-2 proteins from intracellular vesicles into the apical membrane. In this system, we determined the kinetics of induction and recurrence of transcellular osmotic water flow in relation to dDAVP addition and removal, respectively.

Materials and Methods

Expression Construct

For high-level expression of AQP-2, a 900-bp *Eco*RI fragment containing the entire coding region of human *AQP-2* cDNA (11) was blunted and cloned into the blunted *Bgl*II site of pSG5H (23). *In vivo* expression of AQP-2 cRNA from this construct, named pSG5H*AQP2* (Figure 1), is under control of the simian virus 40 early promoter.

Cell Culture and Transfection

MDCK-high resistance cells were grown in Dulbecco's modified Eagle's medium (DMEM) supplemented with 5% (vol/vol) fetal calf serum at 37°C in 5% CO_2. Transfection of 10 μg of *Xba*I-linearized pSG5H*AQP2* mixed with 10 μg of sheared human carrier DNA was realized via calcium phosphate precipitation (24), as described in detail (23). Twenty-four hours after transfection and subsequently every 3 to 4 d, the cells were fed with medium containing 75 μg/ml hygromycin B (ICN Biochemicals, Costa Mesa, CA). Ten to fourteen days after transfection, individual colonies were selected and expanded.

Northern Blot Analysis

Five μg of total RNA, isolated according to the method of Chomczynski and Sacchi (25), was resolved in a 2.2 M formaldehyde, 1% (wt/vol) agarose gel, transferred to a nylon membrane, and ultraviolet cross-linked. Hybridization and washing conditions were as described (26). For normalization, the blot was hybridized with a 1250-bp *Pst*I cDNA fragment coding for rat glyceraldehyde-3-phosphate dehydrogenase (GAPDH) (27).

Immunoblotting

A rat renal medulla was dissected, cut into small pieces, and homogenized in homogenization buffer (Hb; 250 mM sucrose, 10 mM Hepes, pH 7.5, 2 mM $MgCl_2$, 1 mM ethyleneglycol-bis-(β-aminoethyl ether)-*N,N'*-tetra-acetic acid, 1 mM phenylmethyl sulfonyl fluoride, and 5 μg/ml pepstatin) with 0.1% sodium dodecyl sulfate. Native and transfected cells were grown to confluence, scraped, washed twice with phosphate-buffered saline (PBS), and resuspended in Hb. After sonification, protein concentrations were determined with the BioRad protein assay. Immunoblotting of protein equivalents of 6 μg was done as described before (13). To detect AQP-2 proteins, a 1:5000 dilution of affinity-purified rabbit anti-AQP-2 immunoglobulins raised against the 15 C-terminal amino acids of rat AQP-2 (13) was used as a primary antibody, and a 1:5000 diluted affinity-purified goat anti-rabbit IgG antiserum (whole molecule; Sigma Chemical Co., St. Louis, MO) coupled to horseradish peroxidase was used as a secondary antibody. Sites of antigen–antibody reactions were visualized with enhanced chemiluminography according to the manufacturer (Boehringer Mannheim, Mannheim, Germany).

Transcellular Water Transport

The spectroscopic method used to assay for transcellular waterflow was developed by Jovov *et al.* (28) and has been described in detail (23). In brief, area equivalents of 1 cm^2 of confluent layers of cells were seeded onto polycarbonate filters (Costar, Cambridge, MA) with a surface area of 0.33 cm^2. On the second day after seeding, the medium was refreshed, and indomethacin was added to a final concentration of 1×10^{-5} M until the end of the experiments. The next day, the apical and basolateral compartments of the tissue culture chamber were washed with Krebs-Henseleit buffer (KHB) (1.2 mM $MgSO_4$, 128 mM NaCl, 5 mM KCl, 2 mM NaH_2PO_4, 10 mM NaAc, 20 mM Hepes, 1 mM $CaCl_2$, 1 mM L-alanine, 4 mM L-lactate, pH 7.4) and 150 μl of 0.5× KHB containing 30 mg/L phenol red or 800 μl of KHB was added to the apical or basal compartment, respectively. After incubation for 2 h at 37°C, the content of the apical compartment was mixed with a pipette. Two aliquots of 50 μl per insert were put into Eppendorf tubes (for duplicate measurements), diluted with Tris-buffered saline (TBS; 20 mM Tris and 73 mM NaCl, pH 7.6), 2% (wt/vol) extrane (Merck, Darmstadt, Germany) to 600 μl, centrifuged for 5 min, and analyzed for absorbency at 479 nm, the isosbestic point for phenol red (28). From the extinction values at 479 nm, the transported water volume and the osmotic water permeability (Pf, in μm/s) were calculated as described (23). Leaking cell layers, recognized by the presence of phenol red in the liquid taken from the basolateral compartment, were excluded. When indicated, water transport was assayed in the presence of 1×10^{-8} M dDAVP, AVP, or 1×10^{-5} M forskolin. In some experiments, cells were fixed for 5 min in cold 0.15 M cacodylate buffer (pH 7.4) containing 1% (vol/vol) glutaraldehyde and washed twice with KHB before being assayed for osmotic water transport. To determine the sensitivity of water transport to sulfhydryl reagents, the waterflow was assayed in the presence of 3 mM $HgCl_2$ after fixation of the cell layer with glutaraldehyde. To study the induction of transcellular water transport, *AQP-2*-transfected MDCK cells were incubated with dDAVP for different periods, fixed with glutaraldehyde, washed with KHB, and assayed for water transport. To study the reversibility of transcellular water transport, cells were preincubated for 30 min with 1×10^{-8} M dDAVP in DMEM, washed three times with DMEM, incubated for different periods with DMEM with or without 1×10^{-8} M dDAVP, fixed with glutaraldehyde, and assayed for water transport. Unless stated otherwise, all addition of reagents was made to both compartments.

Intracellular cAMP

Cells were seeded and grown to confluence on semipermeable inserts as described above. On the third day, cells were treated for different periods with dDAVP, identical and parallel to experiments in which the induction of transcellular water permeability was determined (see above). After induction, the medium was aspirated and the filters were excised, immediately submerged in 100 μl of 0.2 M HCl, mixed, and stored at −20°C. After three freeze-thaw cycles, lysed cells were centrifuged for 5 min at 10,000 × *g* at 4°C. Next, different dilutions of the supernatant were analyzed for cAMP content with an RIA, as described (29), from which the original intracellular cAMP amounts were calculated.

Immunofluorescence Microscopy

Cells, grown on glass coverslips for 3 d, were incubated for 2 h with DMEM with or without 1×10^{-5} M forskolin, rinsed with ice-cold PBS, fixed for 30 min in 3% (wt/vol) paraformaldehyde in PBS at room temperature, followed by a 20 min incubation in 50 mM NH_4Ac in PBS to quench the fixative. To visualize the apical membrane, glycoproteins at the luminal side were covalently labeled with biotin linker chain-hydrazide (Pierce, Rockford, IL) as described (30). Subsequently, the cells were permeabilized by a 5-min treatment in PBS, 0.2% (wt/vol) sodium dodecyl sulfate, and washed three times with PBS. Potential sites for nonspecific antibody binding were blocked by a 30-min incubation with 10% goat serum in PBS. Subsequently, the coverslips were incubated overnight with a mixture of a 1:100 dilution of affinity-purified rabbit anti-AQP-2 antibodies (13), a 1:2000 dilution of rat anti-mouse E-cadherin (Sigma), and a 1:100 dilution of tetrarhodamine isothiocyanate-coupled extravidin (Sigma) in PBS, 0.2% NaN_3. E-Cadherin is a well known marker for the basolateral membrane. Next, the cells were washed three times in PBS, incubated for 1 h with a 1:100 dilution of affinity-purified goat anti-rabbit IgG coupled to FITC (Sigma) and a 1:100 dilution of affinity-purified Cy-5-conjugated goat anti-rat IgG (Jackson Immunoresearch, West Grove, PA), washed again three times, dehydrated by a 70, 80, 90, and 100% ethanol series and mounted in mowiol 4–88, 2.5% NaN_3. Horizontal extended-focus images and vertical images were obtained with a Bio-Rad MRC-1000 laser scanning confocal imaging system using a 60× oil-immersion objective, a 32-Kalman collection filter, an aperture diaphragm of 2.5, and an axial resolution of 0.14 μm per pixel. The images were contrast-stretched, and a threshold value with pseudocolor was applied. As controls, omission of primary or secondary antibodies revealed no labeling.

Results

Transfection of MDCK-high resistance cells with pSG5H*AQP2* (Figure 1) revealed 44 hygromycin-resistant clones, 14 of which were subjected to Western blot analysis (not shown). A representative clone with ample expression of AQP-2, named wild-type 10 (WT-10), was selected. Northern blot analysis revealed that cells of this clone generated AQP-2 transcripts of the expected size of 1.4 kb, which were not detected in nontransfected MDCK cells (Figure 2A). Immunoblot analysis of proteins from WT-10 cells and rat renal medulla revealed a strong 30-kD signal, corresponding to the molecular mass of nonglycosylated AQP-2 (Figure 2B). In addition, a broad band of 35 to 45 kD (rat medulla) or 40- to 80-kD proteins (WT-10 cells) were detected, which presumably represent glycosylated AQP-2 proteins. No signal was obtained in the lane loaded with proteins of nontransfected MDCK cells.

Analysis of the transcellular osmotic water transport (Figure 3) revealed that the basal Pf of WT-10 cells was about 6 times higher than that of nontransfected MDCK cells. Incubation with dDAVP increased the Pf of WT-10 cells only 1.2 times. Determination of the intracellular cAMP levels showed that the high basal water permeability of WT-10 cells correlated with a surprisingly high basal cAMP level (5.3 ± 0.4 pmol/cm^2 ± SEM; $n = 4$), which could be reduced to undetectable levels after an overnight preincubation with the cyclo-oxygenase inhibitor indomethacin (<1.3 pmol/cm^2). As a result, the basal Pf of indomethacin-pretreated WT-10 cells was only twofold higher than that of untransfected MDCK cells. In combination with indomethacin, dDAVP now increased the Pf value of WT-10 cells 3.5-fold. Addition of forskolin or AVP to both compartments (Figure 3) or AVP to the basolateral compartment only (not shown) revealed Pf values similar to dDAVP-treated WT-10 cells. Similar additions did not change the Pf value of native MDCK cells (Figure 3). In all subsequent experiments, cells were preincubated with indomethacin.

As analyzed by immunofluorescent laser scanning confocal microscopy, the low Pf of nonstimulated WT-10 cells appeared to coincide with a compartmentalized perinuclear localization of AQP-2 within the cell (Figure 4A). However, in the fors-

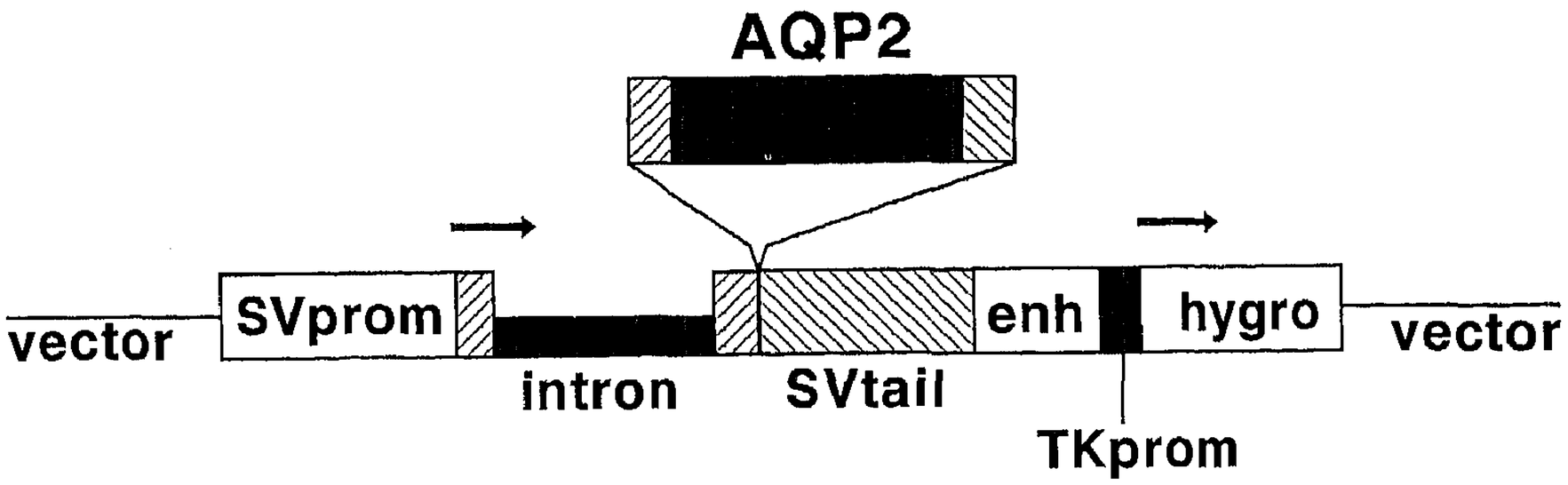

Figure 1. Schematic drawing of expression vector pSG5H*AQP2*. The simian virus 40 (SV40) early promoter (SVprom) and tail (SVtail), the rabbit β-globin intron II (intron), polyoma enhancer (enh), thymidine kinase promoter (TKprom), hygromycin B resistance gene (hygro), and aquaporin (*AQP*)-2 cDNA (AQP2) are indicated. 5′ and 3′ untranslated regions are hatched. The directions of transcription are indicated by arrows.

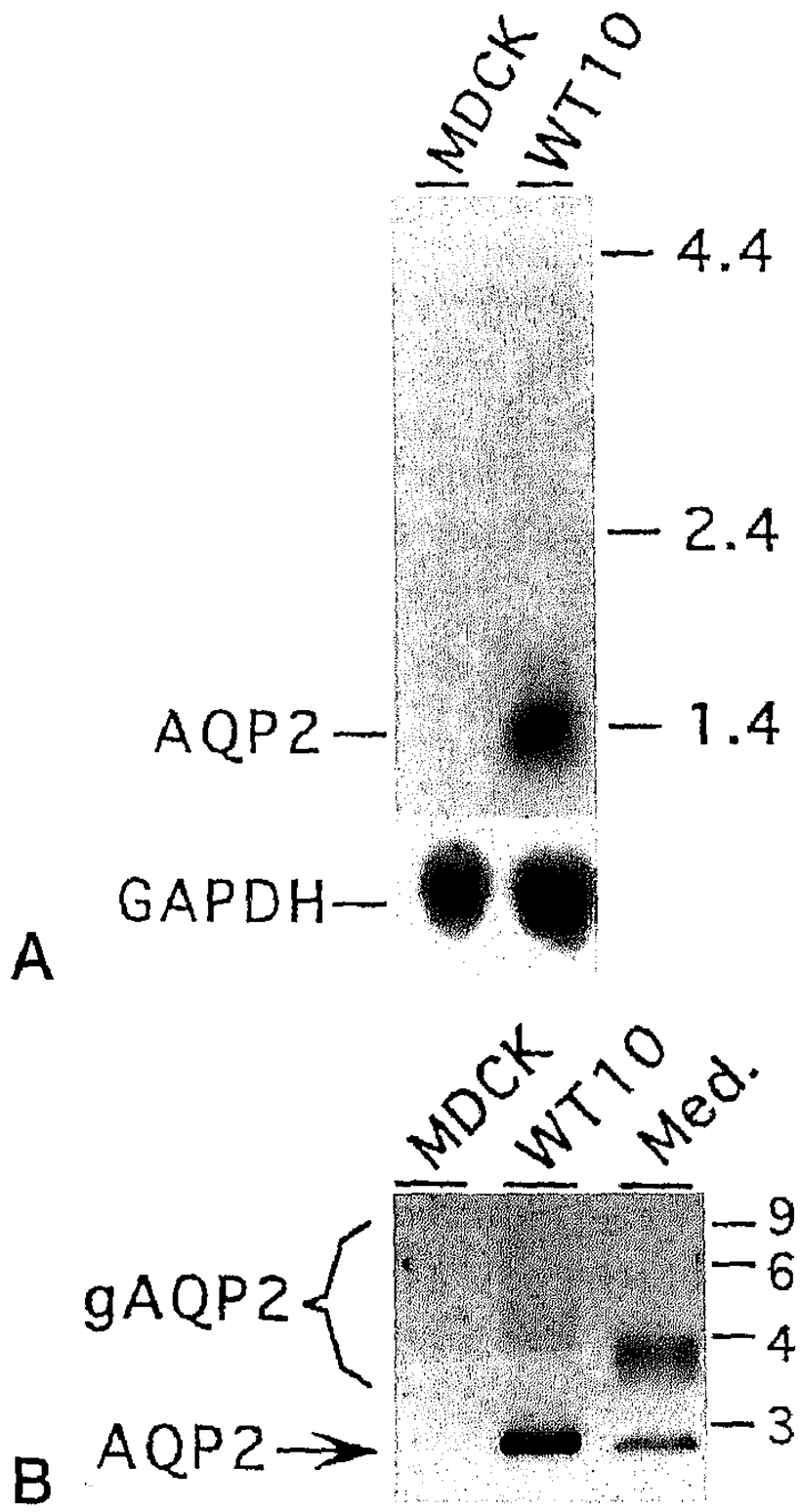

Figure 2. (A) AQP-2 mRNA expression in native Madin-Darby canine kidney (MDCK) cells or *AQP-2*-transfected clone wild-type 10 (WT-10) cells. A total of 5 μg of RNA from these cells was separated on a 2.2 M formaldehyde, 1% (wt/vol) agarose gel and transferred to a nylon membrane. After ultraviolet cross-linking, the blot was hybridized with an [α-^{32}P]-labeled *AQP-2* cDNA probe. For normalization, the blot was hybridized with a rat GAPDH probe. Sizes of marker RNA (in kilobases; Life Technologies) are indicated. (B) AQP-2 expression in native MDCK cells or WT-10 cells. Six-microgram protein equivalents of homogenates of native MDCK cells or WT-10 cells were separated by sodium dodecyl sulfate-polyacrylamide gel electrophoresis and blotted onto a nitrocellulose membrane. AQP-2 proteins were visualized by chemiluminography, using affinity-purified rabbit anti-AQP-2 antibodies as a first antibody and affinity-purified goat anti-rabbit IgG antibodies coupled to horseradish peroxidase as a second antibody. As a positive control, 6 μg of rat renal medulla proteins was loaded. Nonglycosylated AQP-2 (AQP2), the glycosylated form (gAQP2), and the molecular mass (in kilodaltons) of marker proteins (Life Technologies) are indicated.

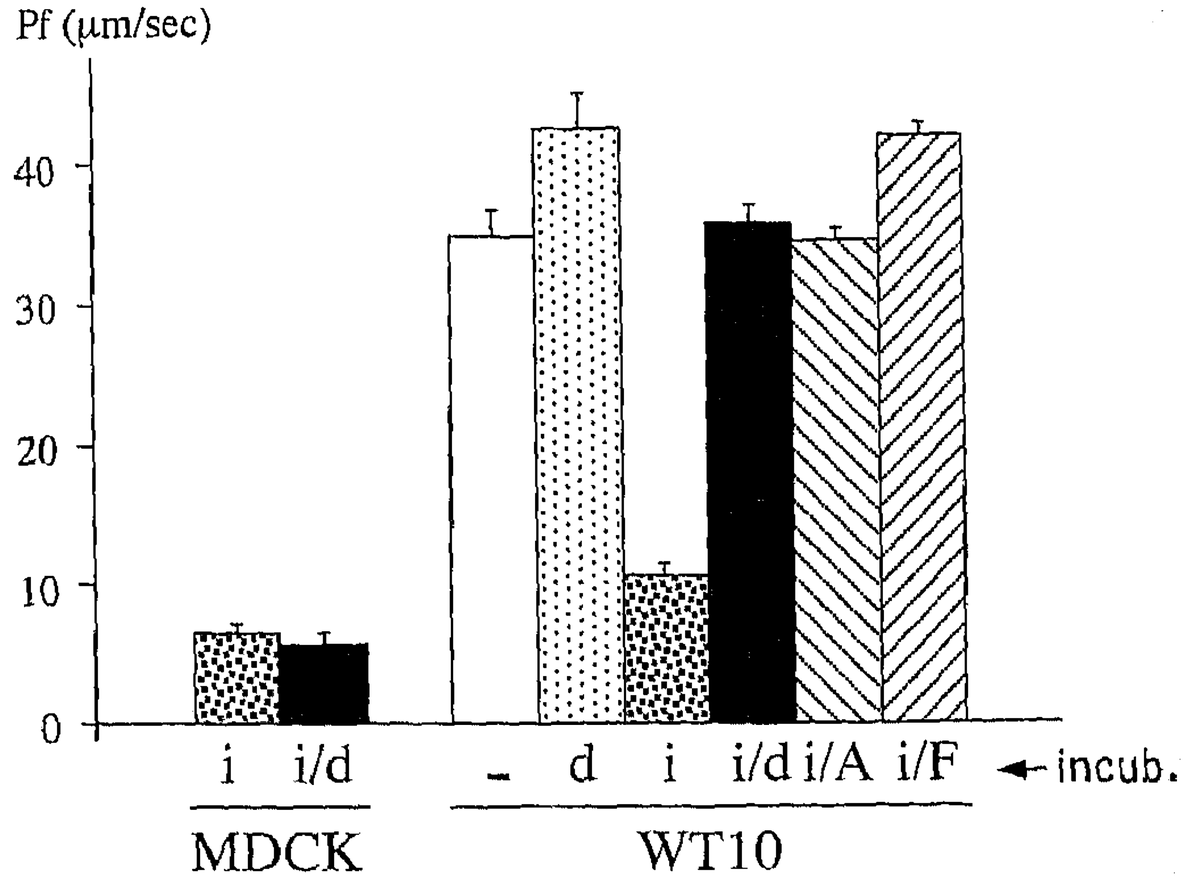

Figure 3. Transcellular osmotic water permeabilities (Pf) of native MDCK or *AQP-2*-transfected clone WT-10 cells. During the assay, the cells were incubated without additives (−) or with 1×10^{-5} M indomethacin (i), 1×10^{-8} M 1-desamino-8-D-arginine vasopressin (dDAVP) (d), 1×10^{-8} M arginine vasopressin (AVP) (A), or 1×10^{-5} M forskolin (F). Pf is expressed in μm/s ± SEM ($n > 10$). Cells assayed in the presence of indomethacin were also preincubated overnight in medium with indomethacin.

kolin-stimulated situation, AQP-2 was homogeneously distributed in the cell (Figure 4B). To determine the distribution with respect to the cell polarization, optical X-Z sections were obtained (Figure 5). In unstimulated WT-10 cells, AQP-2 was in vesicular-like structures dispersed over the entire cell, and predominantly at the apical side, but hardly any AQP-2 was detected in the apical membrane. In forskolin-stimulated WT-10 cells, however, which exhibit a high Pf (Figure 3), nearly all AQP-2 was present in the apical membrane, as concluded from the colocalization of AQP-2 with glycoproteins on the apical surface (Figure 5, B through D). Nontransfected MDCK cells were negative for AQP-2 (Figure 5E).

To study the kinetics and recurrence of the dDAVP-induced increase in transcellular osmosis, fixation of the cells with glutaraldehyde was introduced. Pilot studies revealed that the Pf of WT-10 cells, stimulated with dDAVP after fixation, was not different from nonstimulated WT-10 cells with or without fixation (Figure 6). Although fixation of WT-10 cells, preincubated for 30 min with dDAVP, resulted in a somewhat reduced Pf when compared with nonfixed dDAVP-stimulated WT-10 cells, the Pf value remained nearly 3 times higher than that of nonstimulated WT-10 cells (Figure 6). The dDAVP-induced transcellular water transport across fixed WT-10 cells was Hg-sensitive (Figure 6). Application of $HgCl_2$ to nonfixed dDAVP-treated WT-10 cells resulted in leakage of phenol red to the basolateral compartment, indicative of the toxic effect of $HgCl_2$ on MDCK cells.

The induction of transcellular waterflow was investigated by incubation of WT-10 cells with dDAVP for different periods, followed by fixation with glutaraldehyde and water permeability measurements (Figure 7A). It appeared that within 5 min after addition of dDAVP, the transcellular osmotic water flow doubled. Thirty minutes after dDAVP addition, a maximal Pf value was obtained, which was sustained for at least 1.5 h. In parallel experiments, the intracellular cAMP levels were shown to peak sharply at 5 min after dDAVP admission and subsequently decreased to nearly basal levels within 45 min.

The recurrence of transcellular osmotic waterflow was investigated by incubation of WT-10 cells with dDAVP for 30 min, followed by washout of dDAVP and further incubation of the cells in the presence or absence of dDAVP for different periods (Figure 7B). Incubation with dDAVP after dDAVP

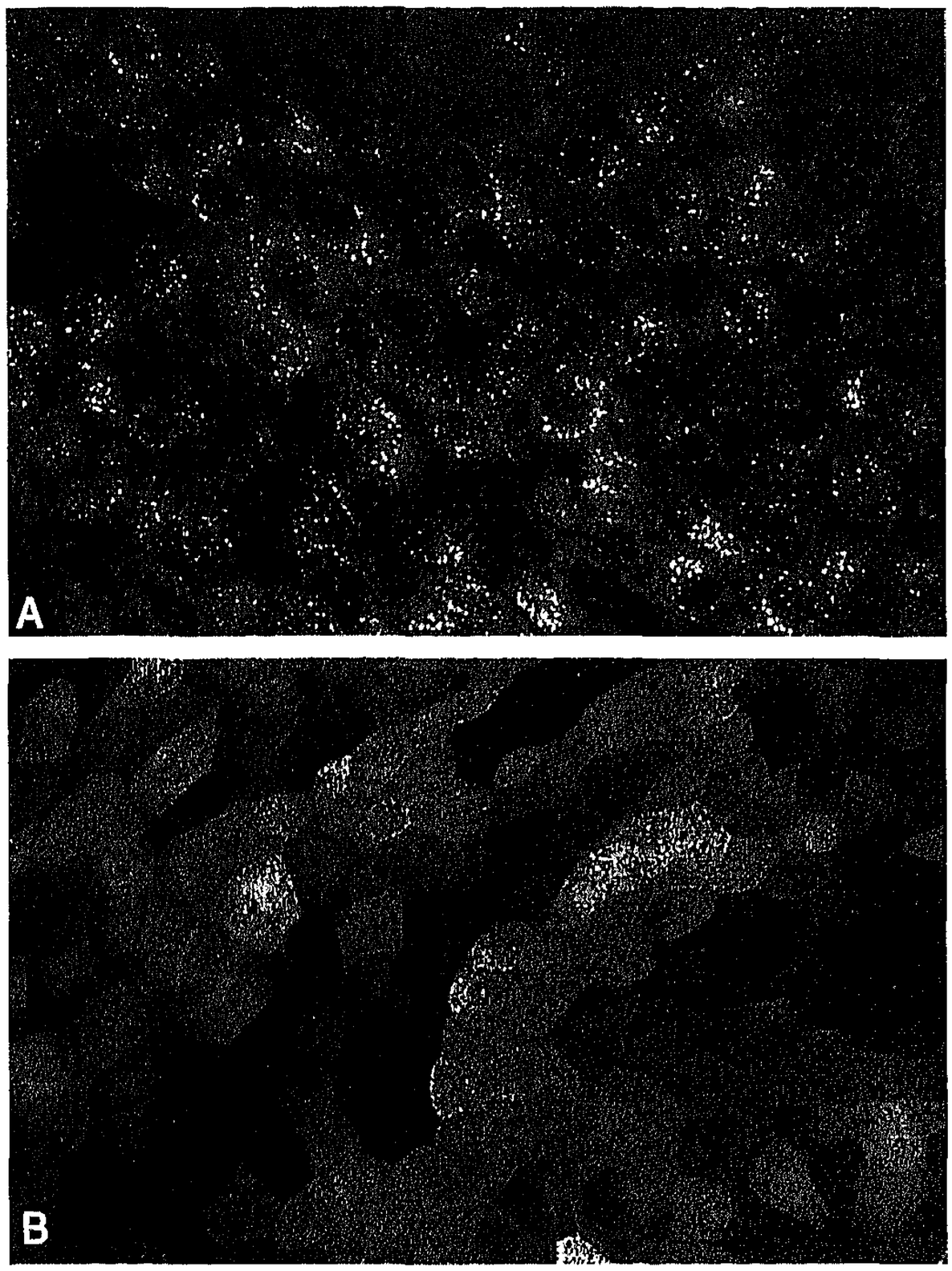

Figure 4. Immunolocalization of AQP-2 in WT-10 cells. WT-10 cells grown on coverslips were incubated for 2 h in DMEM without (A) or with (B) 1×10^{-5} M forskolin and fixed with 3% (wt/vol) paraformaldehyde. After permeabilization, cells were incubated overnight with affinity-purified rabbit anti-AQP-2 antibodies, washed, incubated with affinity-purified goat anti-rabbit IgG coupled to FITC, washed again, dehydrated in an ethanol series, and mounted in mowiol. X-Y optical sections were collected with a Bio-Rad MRC-1000 laser scanning confocal imaging system. Indomethacin was present in the media from 24 h before until the end of the experiment.

preincubation resulted in a sustained high Pf for at least 105 min. In contrast, removal of dDAVP led to a direct but slow decrease in Pf, returning to basal levels within 75 min.

Discussion

The hypothesis that transcellular water permeability in the collecting tubule may be regulated by fusion and endocytosis of vesicles containing water channels was mainly based on early observations that a vasopressin-induced rise in water permeability coincided with the appearance of aggregates of intramembrane particles in the apical membrane (31,32). After the cloning of *AQP-2*, it was shown that AQP-2 resides in intracellular vesicles, which translocate to the apical membrane of collecting duct cells upon vasopressin exposure (7,8). Now, we have generated an AQP-2-expressing MDCK cell line, which to a great extent mimics AVP-regulated and AQP-2-mediated transcellular osmotic water permeability as found in the collecting duct.

The successful generation of an MDCK cell line stably expressing human AQP-2 was proven by Northern and Western blot analyses, which revealed AQP-2-specific signals of the expected sizes, using material from MDCK clone WT-10 cells. The 40- to 80-kD protein bands detected in WT-10 cells presumably constitute glycosylated forms of AQP-2, because with the used AQP-2 antibodies no signal was obtained in native MDCK cells (Figure 2B), and omission of primary or secondary antibodies revealed no signal. These differences in glycosylation might be caused by expression of different subsets of glycosylation enzymes in the two cell types. However, it has been shown that glycosylation of AQP-2 is not essential for proper functioning (4).

Compared with native MDCK cells, WT-10 cells showed a high basal water permeability, which was hardly elevated upon dDAVP treatment (Figure 3). Induction of water transport in collecting duct cells by AVP occurs via cAMP generation, and it is known that prostaglandin E_2, the major cyclo-oxygenase product of the arachidonic acid metabolism in kidney and MDCK cells, can increase intracellular cAMP levels (29,33–35). In the absence of AVP, basolateral and luminal prostaglandin E_2 stimulates rabbit collecting duct water permeability and cAMP production, which is thought to be mediated by adenylyl cyclase-stimulating E-prostanoid $(EP)_2$ or EP_4 receptors (29,34). With WT-10 cells, incubation with the cyclo-oxygenase inhibitor indomethacin indeed lowered the intracellular cAMP level of unstimulated WT-10 cells to undetectable levels, which was accompanied by a 3.5-fold reduction in Pf. The prostaglandin-induced elevated intracellular cAMP levels in MDCK cells might therefore also be mediated by $EP_{2/4}$ receptors. The reduced Pf was almost 2 times higher than that of native MDCK cells, suggesting that in nonstimulated WT-10 cells there is still some AQP-2 present in the apical membrane. The well known inhibitory effect of basolateral prostaglandin E_2 on AVP-mediated water reabsorption in the collecting duct is thought to occur through binding of G_i-coupled $EP_{1/3}$ receptors (34–36). Whether the AVP-mediated transcellular water flow in WT-10 cells is modulated by prostanoids remains to be established.

Incubation of indomethacin-pretreated WT-10 cells with dDAVP, AVP, or forskolin increased the transcellular Pf 3.5-fold (Figure 3). In an AQP-2-transfected human cell line, AVP treatment resulted in a similar elevation of the water permeability of just the apical membrane (20). Compared with collecting tubules (1,37), the 3.5-fold increase in transcellular waterflow in our cells seems rather small. This could be due to low AQP-2 expression levels, but it is most likely due to influences of unstirred layers, which reduce the effective osmotic gradient, since the filter thickness and the fact that the apical and basolateral solutions are essentially unstirred are favorable conditions for solute polarization. Most importantly, however, is the observation that the increase in Pf correlates with a clear translocation of AQP-2 from an intracellular compartment to the apical membrane of WT-10 cells (Figures 4 and 5). Because the Pf of native MDCK cells could not be induced by dDAVP (Figure 3), the dDAVP-induced shift in Pf found in MDCK clone WT-10 can only be explained by the

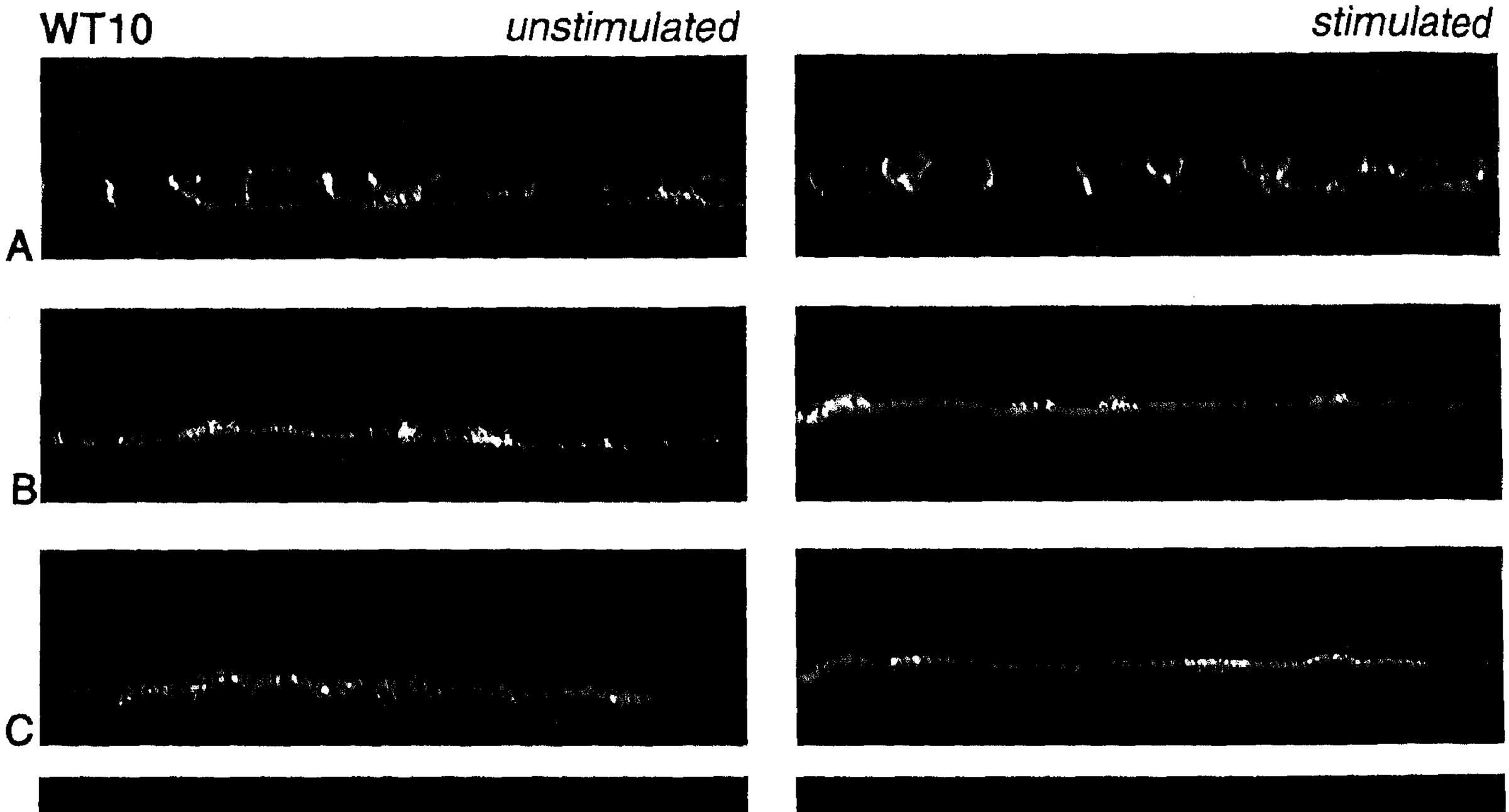

Figure 5. Immunolocalization of AQP-2 in WT-10 cells and MDCK cells. WT-10 (A through D) and MDCK cells (E) were treated without (unstimulated) or with (stimulated) forskolin, fixed, and apically labeled with biotin linker chain-hydrazide. After permeabilization, cells were incubated overnight with affinity-purified rabbit anti-AQP-2 antibodies, rat anti-mouse E-cadherin, and tetrarhodamine isothiocyanate-coupled extravidin. Next, the cells were washed, incubated for 1 h with affinity-purified goat anti-rabbit IgG coupled to FITC and Cy-5-coupled goat anti-rat IgG, washed again, dehydrated in an ethanol series, and mounted in mowiol. X-Z axes images were obtained with a Bio-Rad MRC-1000 laser scanning confocal imaging system. E-Cadherin (A; blue in D and E), apical glycoproteins (B; red in D and E), and AQP-2 (C; green in D and E) are indicated. Indomethacin was present in the media from 24 h before until the end of the experiment.

translocation of AQP-2, possibly in combination with AQP-2 phosphorylation.

In contrast to what occurs in our *AQP-2*-transfected MDCK cells, it was reported that in *AQP-2*-transfected LLC-PK_1 cells, AQP-2 is targeted to the basolateral membrane (18). Although cell-specific routing of AQP-2 cannot be excluded, the misrouting of AQP-2 in LLC-PK_1 cells is presumably caused by the c-*myc* epitope affecting routing information in C-terminus of AQP-2.

The Pf measurements in this study take approximately 2 h. To be able to determine the time course of Pf induction, which occurs in the order of minutes in collecting tubules (37), glutaraldehyde fixation was exploited. Fixation prevented further insertion of AQP-2 molecules into the apical membrane, because incubation of unstimulated cells with dDAVP after fixation revealed no increase in Pf (Figure 6), whereas a 5-min incubation of WT-10 cells with dDAVP already resulted in an increased Pf (Figure 7A). In addition, fixation of dDAVP-treated WT-10 cells resulted in a similar high Pf as nonfixed dDAVP-treated cells. The Pf of fixed dDAVP-treated WT-10 cells could be blocked by mercurials, indicative of the fact that transcellular water permeability is AQP-2-mediated. When $HgCl_2$ was added to nonfixed dDAVP-treated WT-10 cells, phenol red leaked to the basolateral compartment. These latter

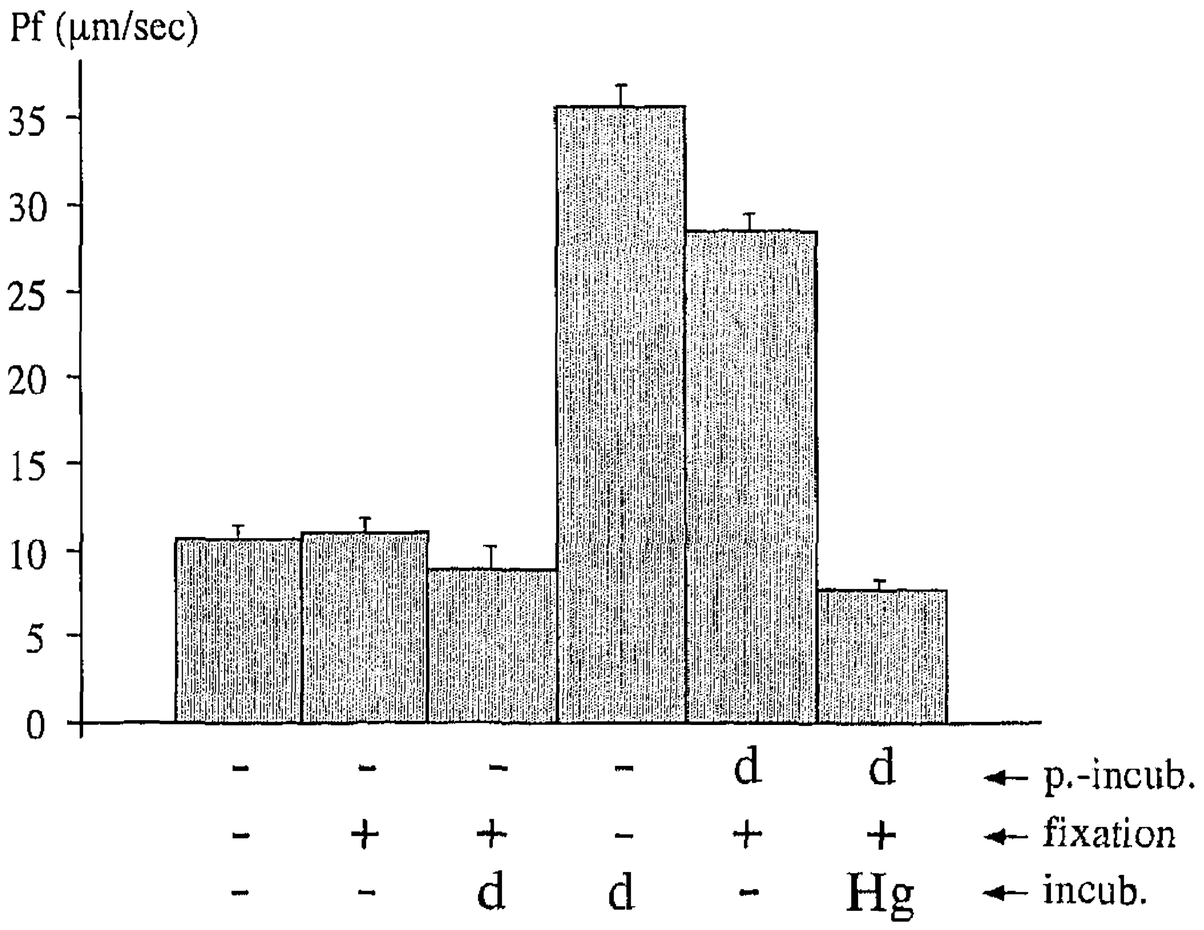

Figure 6. The effect of glutaraldehyde fixation on the transcellular osmotic water permeability (Pf) of *AQP-2*-transfected WT-10 cells. WT-10 cells grown on semipermeable inserts were preincubated for 30 min in Dulbecco's modified Eagle's medium (DMEM) without (−) or with (d) dDAVP, fixed (+) or not fixed (−) with glutaraldehyde, and assayed for transcellular osmotic water transport without additives (−) or after addition of dDAVP (d) or $HgCl_2$ (Hg). The Pf is expressed in μm/s ± SEM ($n > 10$). Indomethacin was present in the media from 24 h before until the end of the experiment.

two observations underscore the fact that fixation of the cells leaves the epithelial barrier intact. From these data, we concluded that this fixation technique, which has been shown to preserve water permeability characteristics of toad urinary bladders, renal descending vasa recta, and AQP-1-transfected cells (23,38,39), is very useful in studying the kinetics of dDAVP-induced water permeation in WT-10 cells.

The transcellular osmotic water permeability of WT-10 cells was doubled within 5 min after addition of dDAVP, reached a plateau value within 30 min, and remained high for at least 1.5 h. The induction of transcellular waterflow coincided with a peak in intracellular cAMP at 5 min after dDAVP admission. Washout of dDAVP, after an incubation time of 30 min, resulted in a slow decrease of the Pf, which reached prestimulated levels 75 min after washout. The periods over which induction and recurrence of the Pf was obtained in WT-10 cells are remarkably similar to the kinetics of AVP-provoked water flow in isolated inner medullary collecting ducts (37). The somewhat slower initial increase in Pf in WT-10 cells may be a consequence of delayed diffusion of dDAVP.

In conclusion, the *AQP-2*-transfected MDCK cells reveal a dDAVP-regulated transcellular osmotic water permeability and translocation of AQP-2, which is similar to vasopressin effects in the collecting duct. Therefore, WT-10 cells provide a good model system to study vasopressin-regulated osmotic water permeability. Furthermore, WT-10 cells might prove useful in unraveling the molecular causes of secondary NDI and in the development of AQP-2-specific diuretics. In addition, analyses of expression in this type of MDCK cells of mutant AQP-2 proteins, as found encoded in NDI patients, is likely to provide the molecular cause of primary NDI.

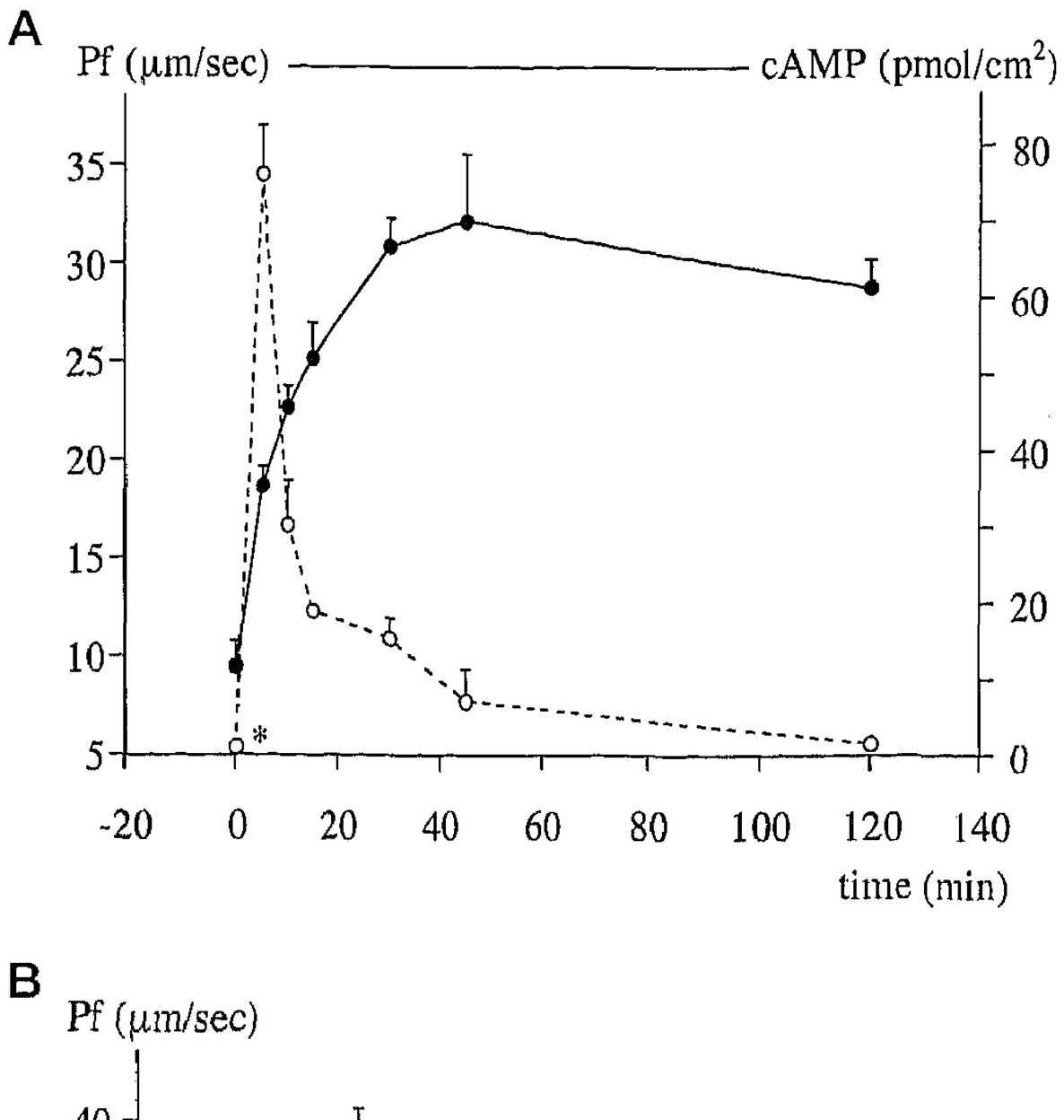

Figure 7. Kinetics of Pf in *AQP-2*-transfected WT-10 cells. (A) Induction of water transport. WT-10 cells grown on semipermeable inserts were incubated for different periods in DMEM containing indomethacin and dDAVP, fixed with glutaraldehyde, and assayed for transcellular osmotic water flow (filled circles). Intracellular cAMP levels at corresponding time points are indicated by open circles. A cAMP value below detection level is indicated by the asterisk. (B) Recurrence of water transport. WT-10 cells grown on semipermeable inserts were preincubated for 30 min with dDAVP in DMEM, washed three times with DMEM, incubated for different periods in DMEM with (closed circles) or without (open circles) dDAVP, fixed with glutaraldehyde, and assayed for water transport. WT-10 cells not treated with dDAVP were taken as negative controls (open squares). The Pf and cAMP values are expressed in μm/s ± SEM and pmol/cm^2 ± SEM, respectively ($n = 6$). Indomethacin was present in the media from 24 h before until the end of the experiment.

Acknowledgments

We acknowledge Huib Croes and Hans Smits for technical advice with the laser scanning confocal microscopy and Maarten de Jong for

technical assistance with the cAMP assay. This study was supported by Grants C93.1299 and C95.5001 from the Dutch Kidney Foundation to Peter M. T. Deen and Johan P. L. Rijss; a fellowship of the Royal Netherlands Academy of Arts and Sciences to Peter M. T. Deen; and Grant NWO-SLW-810-405-16-2 from the Dutch Science Foundation to Sabine M. Mulders.

References

1. van Os CH, Deen PMT, Dempster JA: Aquaporins: Water selective channels in biological membranes. Molecular structure and tissue distribution. *Biochim Biophys Acta* 1197: 291–309, 1994
2. Agre P, Brown D, Nielsen S: Aquaporin water channels: Unanswered questions and unresolved controversies. *Curr Opin Cell Biol* 7: 472–483, 1995
3. Preston GM, Jung JS, Guggino WB, Agre P: The mercury-sensitive residue at cysteine 189 in the CHIP28 water channel. *J Biol Chem* 268: 17–20, 1993
4. Bai LQ, Fushimi K, Sasaki S, Marumo F: Structure of aquaporin-2 vasopressin water channel. *J Biol Chem* 271: 5171–5176, 1996
5. Nielsen S, Agre P: The aquaporin family of water channels in kidney. *Kidney Int* 48: 1057–1068, 1995
6. Fushimi K, Uchida S, Hara Y, Hirata Y, Marumo F, Sasaki S: Cloning and expression of apical membrane water channel of rat kidney collecting tubule. *Nature* 361: 549–552, 1993
7. Hayashi M, Sasaki S, Tsuganezawa H, Mokawa T, Kitajima W, Konishi K, Fushimi K, Marumo F, Saruta T: Expression and distribution of aquaporin of collecting duct are regulated by vasopressin V2 receptor in rat kidney. *J Clin Invest* 94: 1778–1783, 1994
8. Nielsen S, Chou CL, Marples D, Christensen EI, Kishore BK, Knepper MA: Vasopressin increases water permeability of kidney collecting duct by inducing translocation of aquaporin-CD water channels to plasma membrane. *Proc Natl Acad Sci USA* 92: 1013–1017, 1995
9. Ishibashi K, Sasaki S, Fushimi K, Uchida S, Kuwahara M, Saito H, Furukawa T, Nakajima K, Yamaguchi Y, Gojobori T: Molecular cloning and expression of a member of the aquaporin family with permeability to glycerol and urea in addition to water expressed at the basolateral membrane of kidney collecting duct cells. *Proc Natl Acad Sci USA* 91: 6269–6273, 1994
10. Jung JS, Bhat RV, Preston GM, Guggino WB, Baraban JM, Agre P: Molecular characterization of an aquaporin cDNA from brain: Candidate osmoreceptor and regulator of water balance. *Proc Natl Acad Sci USA* 91: 13052–13056, 1994
11. Deen PMT, Verdijk MAJ, Knoers NVAM, Wieringa B, Monnens LAH, Van Os CH, Van Oost BA: Requirement of human renal water channel aquaporin-2 for vasopressin-dependent concentration of urine. *Science* 264: 92–95, 1994
12. Van Lieburg AF, Verdijk MAJ, Knoers NVAM, Van Essen AJ, Proesman W, Mallmann R, Monnens LAH, Van Oost BA, Van Os CH, Deen PMT: Patients with autosomal nephrogenic diabetes insipidus homozygous for mutations in the aquaporin 2 water-channel gene. *Am J Hum Genet* 55: 648–652, 1994
13. Deen PMT, Croes H, van Aubel RAMH, Ginsel LA, van Os CH: Water channels encoded by mutant aquaporin-2 genes in nephrogenic diabetes insipidus are impaired in their cellular routing. *J Clin Invest* 95: 2291–2296, 1995
14. Mulders SM, Knoers NVAM, van Lieburg AF, Monnens LAH, Leumann E, Wühl E, Schober E, Rijss JPL, van Os CH, Deen PMT: New mutations in the AQP2 gene in nephrogenic diabetes insipidus resulting in functional but misrouted water channels. *J Am Soc Nephrol* 8: 242–248, 1997
15. Marples D, Christensen S, Christensen EI, Ottosen PD, Nielsen S: Lithium-induced downregulation of aquaporin-2 water channel expression in rat kidney medulla. *J Clin Invest* 95: 1838–1845, 1995
16. Marples D, Frokiaer J, Dorup J, Knepper MA, Nielsen S: Hypokalemia-induced downregulation of aquaporin-2 water channel expression in rat kidney medulla and cortex. *J Clin Invest* 97: 1960–1968, 1996
17. Frokiaer J, Marples D, Knepper MA, Nielsen S: Bilateral ureteral obstruction downregulates expression of vasopressin-sensitive AQP-2 water channel in rat kidney. *Am J Physiol* 39: F657–F668, 1996
18. Katsura T, Verbavatz JM, Farinas J, Ma T, Ausiello DA, Verkman AS, Brown D: Constitutive and regulated membrane expression of aquaporin 1 and aquaporin 2 water channels in stably transfected LLC-PK1 epithelial cells. *Proc Natl Acad Sci USA* 92: 7212–7216, 1995
19. Katsura T, Ausiello DA, Brown D: Direct demonstration of aquaporin-2 water channel recycling in stably transfected LLC-PK1 epithelial cells. *Am J Physiol* 39: F548–F553, 1996
20. Oksche A, Schulein R, Rutz C, Liebenhoff U, Dickson J, Muller H, Birnbaumer M, Rosenthal W: Vasopressin V2 receptor mutants that cause X-linked nephrogenic diabetes insipidus: Analysis of expression, processing, and function. *Mol Pharmacol* 50: 820–828, 1996
21. Richardson JC, Scalera V, Simmons NL: Identification of two strains of MDCK cells which resemble separate nephron tubule segments. *Biochim Biophys Acta* 673: 26–36, 1981
22. Simmons NL, Tivey DR: The effect of hyperosmotic challenge upon ion transport in cultured renal epithelial layers (MDCK). *Pflügers Arch* 421: 503–509, 1992
23. Deen PMT, Nielsen S, Bindels RJM, Van Os CH: Apical and basolateral expression of aquaporin-1 in transfected MDCK and LLC-PK cells and functional evaluation of transcellular osmotic water permeabilities. *Pflügers Arch* 433: 780–787, 1997
24. Graham FL, Eb AJ: A new technique for the assay of infectivity of human adenovirus 5 DNA. *Virology* 52: 456–467, 1973
25. Chomczynski P, Sacchi N: Single-step method of RNA isolation by acid guanidinium thiocyanate-phenol-chloroform extraction. *Anal Biochem* 162: 156–159, 1987
26. Deen PM, Dempster JA, Wieringa B, Van Os CH: Isolation of a cDNA for rat CHIP28 water channel: High mRNA expression in kidney cortex and inner medulla. *Biochem Biophys Res Commun* 188: 1267–1273, 1992
27. Fort P, Marty L, Piechaczyk M, El Sabrouty S, Dani C, Jeanteur P, Blanchard JM: Various rat adult tissues express only one major mRNA species from the glyceraldehyde-3-phosphate-dehydrogenase multigenic family. *Nucleic Acids Res* 13: 1431–1442, 1985
28. Jovov B, Wills NK, Lewis SA: A spectroscopic method for assessing confluence of epithelial cell. *Am J Physiol* 261: C1196–C1203, 1991
29. van Baal J, de Jong MD, Zijlstra FJ, Willems PHGM, Bindels RJM: Endogenously produced prostanoids stimulate calcium reabsorption in the rabbit cortical collecting system. *J Physiol (Lond)* 497: 229–239, 1996
30. Lisanti MP, Le Bivic A, Sargiacomo M, Rodriguez Boulan E: Steady-state distribution and biogenesis of endogenous Madin-Darby canine kidney glycoproteins: Evidence for intracellular

sorting and polarized cell surface delivery. *J Cell Biol* 109: 2117–2127, 1989
31. Wade JB, Stetson DL, Lewis SA: ADH action: Evidence for a membrane shuttle mechanism. *Ann NY Acad Sci* 372: 106–117, 1981
32. Harmanci MC, Kachadorian WA, Valtin H, Discala VA: Antidiuretic hormone-induced intramembranous alterations in mammalian collecting ducts. *Am J Physiol* 235: 440–443, 1978
33. Hassid A: Modulation of cyclic 3′5′-adenosine monophosphate in cultured renal (MDCK) cells by endogenous prostaglandins. *J Cell Physiol* 116: 297–302, 1983
34. Sakairi Y, Jacobson HR, Noland TD, Breyer MD: Luminal prostaglandin E receptors regulate salt and water transport in rabbit cortical collecting duct. *Am J Physiol* 38: F257–F265, 1995
35. Bonvalet JP, Pradelles P, Farman N: Segmental synthesis and actions of prostaglandins along the nephron. *Am J Physiol* 253: F377–F387, 1987
36. Breyer MD, Ando Y: Hormonal signaling and regulation of salt and water transport in the collecting duct. *Annu Rev Physiol* 56: 711–739, 1994
37. Nielsen S, Knepper MA: Vasopressin activates collecting duct urea transporters and water channels by distinct physical processes. *Am J Physiol* 265: F204–F213, 1993
38. Nielsen S, Pallone T, Smith BL, Christensen EI, Agre P, Maunsbach AB: Aquaporin-1 water channels in short and long loop descending thin limbs and in descending vasa recta in rat kidney. *Am J Physiol* 268: F1023–F1037, 1995
39. Wade JB, Kachadorian WA: Cytochalasin B inhibition of toad bladder apical membrane responses to ADH. *Am J Physiol* 255: C526–C530, 1988